RSC Advances

PAPER

View Article Online
View Journal | View Issue

Cite this: *RSC Adv.*, 2020, **10**, 14694

Strategy to design a smart photocleavable and pH sensitive chitosan based hydrogel through a novel crosslinker: a potential vehicle for controlled drug delivery†

Safiya Nisar,[a] Ashiq Hussain Pandit,[b] Li-Fang Wang*[cd] and Sunita Rattan *[a]

Received 9th December 2019
Accepted 15th March 2020

DOI: 10.1039/c9ra10333c

rsc.li/rsc-advances

We report herein the synthesis of a novel photocleavable crosslinker, 4-formylphenyl 4-((4-formylphenoxy) methyl)-3-nitrobenzoate (CHO–ONB–CHO) and its joining with amine-based polysaccharides, *viz.* chitosan, resulting in the formation of a dual stimuli-responsive (ONB–chitosan) hydrogel having UV- and pH-responsive sites. The detailed mechanism for the formation of CHO–ONB–CHO and ONB–chitosan hydrogel is proposed. The (CHO–ONB–CHO) crosslinker was characterized using ^{1}H-NMR, LCMS and UV-visible spectroscopy. The dual responsive hydrogel is characterized by FTIR, SEM, XRD, DSC and TGA. The crosslinked hydrogel displayed mechanical robustness with a storage modulus of about 1741 pa. The pH-responsiveness of the hydrogel was studied *via* equilibrium swelling studies in various pH media at 37 °C. The photocleavable behavior of the crosslinker was observed in the UV-absorption range of 310–340 nm and the hydrogel exhibited maximum swelling at pH 5.7. The higher swelling of the hydrogel in acidic conditions and its photo-responsiveness can be exploited for the controlled, temporal and spatial release of therapeutic drugs at any inflammatory areas with acidic environments. It was observed that the hydrogel exhibited higher drug release at pH 5.7 than at pH 7.4.

Introduction

Hydrogels have been studied for decades for their outstanding properties of tunability, specificity, and even the ability to respond to environmental conditions making them excellent candidates for drug delivery applications.[1,2] As new drug delivery systems are being developed, they attract growing attention for their extensive applicability in, for example, loading of anticancer drugs, protein drugs and gene drugs, and in their numerous ways of administration *viz.*, nasal, intravenous, ocular and oral.

Though, considerable progress has been made, only a few of the targeting systems have achieved an optimal outcome. The controlled delivery of therapeutic payloads in a disease-, time- and site-specific manner across the physiological pathways remains an unsettled challenge. This challenge is chiefly bothersome in the fighting of various diseases mainly cancers since majority of the chemotherapeutic drugs proposed for the treatment of benign and metastasized cancers are fairly non-aqueous with narrow therapeutic indices.[3] Therefore, the researchers around the world are striving for potential materials with both wide-ranging efficacy and improved specificity.[4] In this regard, development of multi-responsive hydrogels emerges as a potent approach to obtain favorable pharmacokinetics. These materials are often referred to as 'smart' or biomimetic materials.[5] Such fourth generation biomaterials respond to the local environment of the bio-compartment or to the application of external stimuli, thus, growing into sophisticated systems that respond to the specific stimuli.[6] These biomaterials comprise of composites, networks or hydrogels that respond to certain environmental stimuli *viz.*, pH, light, temperature, redox, electric or magnetic field, analyte concentrations.[4,7,8]

Among dual stimulus-responsive drug delivery systems the most studied nanosystems are the pH and temperature-responsive systems.[9–11] Other dual responsive systems studied are pH and redox-sensitive,[12–14] pH and magnetic responsive systems[15,16] and redox and temperature responsive nanoparticles.[17–19] To the best of our knowledge, no work is reported on UV and pH responsive hydrogels which can be exploited for controlled and targeted release of drug at the site of the tumour.

[a]*Amity Institute of Applied Sciences, Amity University, Sector-125, Noida 201303, India. E-mail: srattan@amity.edu*

[b]*Materials Research Laboratory, Department of Chemistry, Jamia Millia Islamia, New Delhi-110025, India*

[c]*Department of Medicinal and Applied Chemistry, College of Life Sciences, Kaohsiung Medical University, Kaohsiung 807, Taiwan. E-mail: lfwang@kmu.edu.tw*

[d]*Department of Medical Research, Kaohsiung Medical University Hospital, Kaohsiung 807, Taiwan*

† Electronic supplementary information (ESI) available. See DOI: 10.1039/c9ra10333c

Taking advantage of slightly acidic cancerous tissue environments (pH 6.0–7.0), endosomes (pH 4.5–6.0) and lysosomes (pH 4.5–4.8) compared to body pH of 7.4 in the non-cancerous tissues and blood, chitosan based stimuli-sensitive hydrogels are being designed and enhanced to release drugs in the tumor site and/or endo/lysosomal compartments[20,21] through the internal stimulus (pH). Further, light (UV) sensitive moiety in the chitosan crosslinking will be used to have the temporal and spatial control of the drug release.[22] Light as external stimulus has drawn special focus because of its tunable properties which can lead to the release of a range of drugs by photodegradation of photosensitive moieties (Scheme 1). It gives us the control of where and when the drug is to be released leading to the efficient drug delivery.[23] Therefore, in this work we aim to design the novel chitosan hydrogel-based system which is dual stimuli-responsive. Chitosan, a structural polysaccharide (Fig. 1) generally found in crustaceans, lower plants and insects. It's a cationic polymer (β-1-4 glucosidic linkage), a major product attained from the chitin alkaline deacetylation.[24] It is generally considered as biocompatible, nontoxic, nonimmunogenic, polymer consistent with the done *in vitro* and *in vivo* studies and is biodegradable and absorbable by many enzymes in the body of a human being.[25,26] For the above properties, chitosan has widely been utilized as a matrix of microparticulate and crosslinked systems for the encapsulation, loading and release of the payloads.[27,28] An extensive research for the development, preparation and crosslinking methods and their interactions within the hydrogels has been carried out by researchers.[29–31] The crosslinking of the crosslinkers is largely affected by the type and the functionalities of the polymer, in this case chitosan.[32] In the present work, a novel photocleavable crosslinker is synthesized and used, which on crosslinking with chitosan introduces pH responsiveness in addition to the response towards UV light. The pH-sensitive swelling and release of the payloads in such hydrogels usually occurs by diffusion through the porous networks.[33] Thus, ionically and covalently crosslinked chitosan hydrogels can be regarded as decent aspirants for the drug delivery applications.

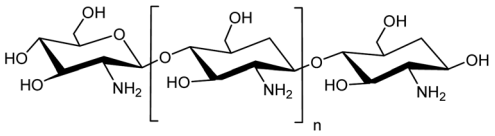

Fig. 1 Chemical structure of chitosan.

In this work, attempts have been made to design a dual stimuli hydrogel through a novel photocleavable crosslinker, 4-formylphenyl 4-((4-formylphenoxy)methyl)-3-nitrobenzoate (CHO–ONB–CHO), which has been used to functionalize chitosan to fabricate the dual stimuli-responsive hydrogel (ONB–chitosan). The dual stimuli (pH and light) responsive hydrogel that swell, dissolve or collapse in response to an internal stimulus (pH) or external stimulus (light), can be used to enhance the drug release at the target site. The higher swelling of the hydrogel at acidic pH and the photo-responsiveness can be exploited for the controlled, temporal and spatial release of the therapeutic drugs at cancer-sites with acidic environments.

Experimental

Materials

4-(Bromomethyl)-3-nitrobenzoic acid (97%), 4-hydroxybenzaldehyde (98%), *N*,*N*′-dicyclohexylcarbodiimide (DCC, 99%), 4-(dimethylamino)pyridine (DMAP, 99%) were purchased from Alfa Aesar. Potassium carbonate (99.995%) and chitosan (75% deacetylation) were obtained from Sigma-Aldrich and Loba Chemie respectively. Acetic acid (99–100%) and doxorubicin hydrochloride (98%) were procured from Merck. Aluminium powder (99.5%) and magnesium silicate were acquired from Kemphasol and Spectrochem respectively. Sodium hydroxide, 2,2′,2″,2‴-(ethane-1,2-diyldinitrilo)tetraacetic acid (EDTA) were procured from Fisher Scientific.

Synthetic procedures

Synthesis of 4-formylphenyl 4-((4-formylphenoxy)methyl)-3-nitrobenzoate (CHO–ONB–CHO). The first step in synthesis

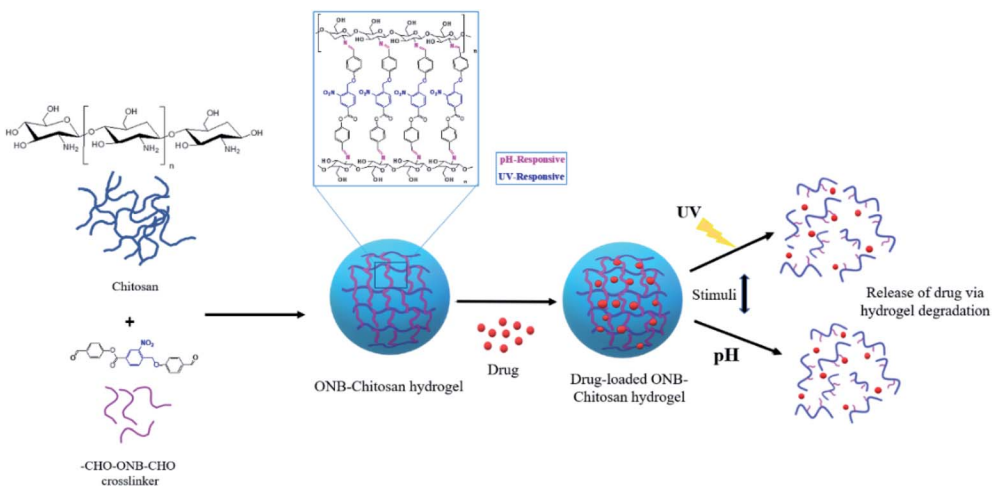

Scheme 1 Schematic representation of photocleavable and pH-responsive hydrogel proposed for drug delivery applications.

the crosslinker is the synthesis of 4-formylphenyl 4-(bromomethyl)-3-nitrobenzoate (Scheme 2).

4-(Bromomethyl)-3-nitrobenzoic acid (2.9 g, 11.15 mmol), was dissolved in dry THF (70 mL) and DMAP (0.64 g, 5.23 mmol) was added and stirred for 10 min. Then DCC (2.2 g, 10.66 mmol) was added and further stirred for 10 min. Finally, 4-hydroxybenzaldehyde (1.0 g, 8.19 mmol), was added to the reaction mixture and stirred at room temperature for 16 h.[34] After confirming the completion of reaction by TLC, the reaction mixture was quenched with water (100 mL) and transferred into a glass separating funnel and the compound was extracted into ethyl acetate (2 × 100 mL). The combined organic layers were washed with NaCl solution (100 mL) and it was dried on anhyd. Na_2SO_4 and the solvent was removed on rotary evaporator, the resulting crude product was washed with diethyl ether (2 × 50 mL) and *n*-pentane (2 × 30 mL), the solvent was decanted and dried under high vacuum, affording CHO–ONB–Br as white solid.

4-Hydroxybenzaldehyde (0.61 g, 5.00 mmol), was dissolved in dry acetone (15 mL) and K_2CO_3 (2.10 g, 15.19 mmol), was added, stirred for 15 min. Then –CHO–ONB–Br (1.0 g, 2.74 mmol), was added and further stirred the reaction mixture at room temperature for 12 h. After determining completion of the reaction by TLC, acetone was removed using rotary evaporator. The resulting residual crude was dissolved in water and transferred into a separating funnel and extracted with ethyl acetate (2 × 100 mL). The separated organic phase was dried over Na_2SO_4 to remove the moisture, the solvent was removed by rotavapor to get crude compound.[35] Then column chromatography was used for purification by using silica gel (75–200 mesh), the solvents such as *n*-hexane and ethyl acetate as eluents affording CHO–ONB–CHO appears as pale yellow solid (Scheme 2). Yield 0.15 g (22.38%).

Preparation of CHO–ONB–CHO crosslinked hydrogels. To prepare the ONB-crosslinked chitosan hydrogel, chitosan (2% w/v) was dissolved in aqueous acetic acid (3% v/v). This solution was added and mixed with magnesium silicate (0.5% w/v) and aluminum powder (0.03%). The above solution was added to 300 mL of NaOH (2 M) solution in a dropwise manner which leads to the formation of microspheres releasing hydrogen. This solution was continuously stirred for 1 hour at room temperature. The resultant microspheres were repeatedly washed with water and then transferred to EDTA solution (0.01 M). This solution was stirred for 20 min.[36]

The synthesized crosslinker (0.1 g) was dissolved in 10 mL of acetone : water (1 : 4) system. The microspheres prepared above were immersed in the solution for 24 hours and washed with water and then freeze-dried.

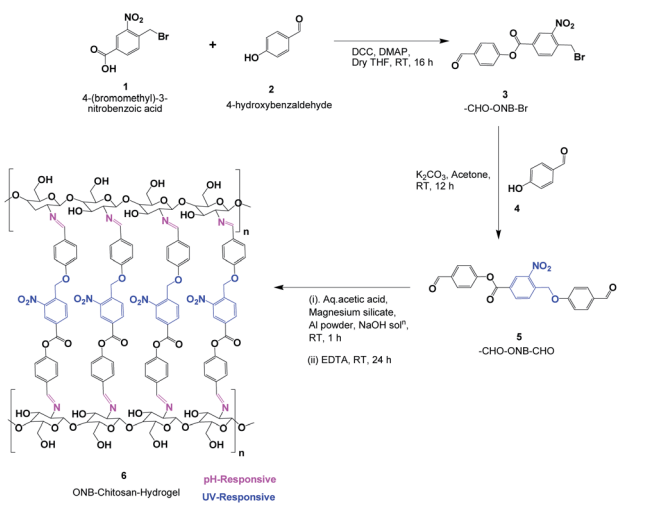

Scheme 2 Synthesis of dual-stimuli responsive ONB–chitosan hydrogel.

Instruments and characterizations

Nuclear magnetic resonance (^{1}H-NMR). The ^{1}H-NMR spectra of CHO–ONB–CHO crosslinker and its bromo- (–CHO–ONB–Br) intermediate were recorded on Oxford 200 NMR spectrometer in $CDCl_3$ and DMSO-d_6.

Liquid chromatography-mass spectroscopy (LCMS). LCMS data was analyzed on Schimadzu, LCMS 8045 and the samples were dissolved in THF (1 mg ml^{-1}).

UV responsive nature of crosslinker (CHO–ONB–CHO). The UV sensitivity of prepared crosslinker was determined by the method already reported in literature with slight modification.[37] The crosslinker solution (3 mg in 3 mL THF) was kept in front of UV lamp (Osram, ULTRA-VITALUX, 300 W) for 10 min. The distance of the crosslinker solution from the UV lamp was maintained at 20 cm. After 0.5, 2, 5, 7, 10 min, the crosslinker sample solution was taken out and examined with the help of UV-visible spectroscopy (Agilent 8453). The UV sensitivity of crosslinker was investigated by changes in the CHO–ONB–CHO absorbance spectrum.

Scanning electron microscopy (SEM) analysis. SEM micrographs of the pristine chitosan and prepared dried hydrogels were taken using Zeiss Evo 18.

Fourier-transform infrared spectroscopy (FTIR). FTIR spectra was recorded for pristine chitosan and the ONB–chitosan hydrogel on PerkinElmer Cetus Instruments, Norwalk.

Crystallographic studies (XRD). XRD patterns of chitosan and crosslinked hydrogels were recorded using Burker D8 Advance Diffractometer.

Thermal gravimetric analysis/differential scanning calorimetry (TGA/DSC). TG/DSC studies were done on STA, Linseis, USA, with a sample size of 3.5–5 mg at a heating rate of 10 °C min^{-1} for temperature ranging from ambient to 800 °C.

Contact angle analysis. Contact angle (CA Analyzer, SEO optics) analysis was done to observe the hydrophobicity of the ONB–chitosan hydrogels compared to that of chitosan. The dried hydrogel microspheres were cut into 2 × 2 cm blocks with the help of surgical blade and then mounted on glass strips.

pH-studies swelling characteristics and swelling kinetics

pH-studies. To investigate the sensitivity of the prepared hydrogels at various pHs, swelling ratio (SR) of the hydrogels was calculated and studied using various buffer solutions (PBS). The freeze-dried hydrogels were initially weighed and immersed in 20 mL PBS solutions of pH 2.1, 5.7 and 7.4 at 37 °C. The

swollen samples were taken out at predetermined time intervals from the buffer solutions, the excess medium on the surface of the hydrogels removed with blotting paper and weighed afterwards. Swelling ratio (SR (%)) was calculated using below equation:

$$\text{SR } (\%) = (W_t - W_0)/W_0 \quad (1)$$

where W_0 is the initial weight of the dried hydrogel and W_t is the weight of the hydrogel at different time intervals.

Swelling kinetics. For the swelling kinetics study, first- and second-order kinetic models were measured using Ritger–Peppas model (eqn (2)).[38] To analyze the mechanism of swelling, defined by the following equation:

$$M_t/M_{eq} = kt^n \quad (2)$$

where M_t & M_{eq} is the amount of water absorbed at time t and at equilibrium respectively, and M_t/M_{eq} is the fractional swelling of the hydrogel in time t, k is the characteristic constant of the hydrogel and the value of the n is the characteristic exponent that defines the mechanism of water transport. The graph plotted between $\log(M_t/M_{eq})$ *vs.* $\log t$, the values of n and k are given by the slope and intercept of the plot respectively. The value of $n \leq 0.45$ implies Fickian diffusion, the value of $n > 0.89$ signifies the Case II diffusion and the value of $0.45 < n < 0.89$ between 0.5 and 1 indicates non-Fickian or anomalous diffusion.

Mechanical properties of ONB–chitosan hydrogel. The rheological studies such as storage modulus (G') and loss modulus (G'') of crosslinked hydrogel was investigated using Anton Peer rheometer (Japan, MCR, 101). The hydrogel was cut into circular shaped disc of 15 mm diameter and then analyzed at room temperature in the frequency range of 0–70 Hz.

***In vitro* drug loading and release studies of ONB–chitosan hydrogel.** The loading of dox into the crosslinked hydrogel matrix was conducted by submerging the hydrogels of know weight (35 mg) in 25 mL of buffer solution of pH 7.4 and 5.5 containing dox (3 mg mL^{-1}). After attainment of swelling equilibrium, these loaded hydrogels were separated from the drug solution, thoroughly washed with PBS and then dried at 30 °C until their weight became constant. The loading of dox was achieved after 72 h when the colour of hydrogels changed to orange (Fig. 3a and b). The loading efficiency was calculated using the equation given below.

$$\text{dox loading}(\%) = \frac{\text{Weight of loaded dox}}{\text{Hydrogels containing dox}} \times 100$$

The dox release studies were carried out by immersing the dox loaded hydrogel in a phosphate buffer solution of pH 5.7 and 7.4 and at room temperature. After, certain intervals of time, the amount of dox released was investigated with the help of UV-visible spectrophotometer (λ_{max} = 485 nm). The dox release from hydrogel was compared with quantity of free dox released standard calibration curve. The dox release studies was investigated in triplicates and their average values were considered applying following equation.

$$\%\text{ release of dox} = [\text{concentration} \times \text{dissolution bath volume} \times \text{dilution factor}]/1000$$

Results and discussions

Synthesis and characterization of the CHO–ONB–CHO

The 4-formylphenyl 4-((4-formylphenoxy)methyl)-3-nitrobenzoate (CHO–ONB–CHO) crosslinked chitosan hydrogels were prepared following a three-step procedure (Scheme 2). The first step of the Scheme 2 involved the synthesis of 4-formylphenyl 4-(bromomethyl)-3-nitrobenzoate (–CHO–ONB–Br) through esterification of 4-(bromomethyl)-3-nitrobenzoic acid with 4-hydroxybenzaldehyde using DCC and DMAP.[34] The resultant bromo-product (–CHO–ONB–Br) acts as a reactant for the next step which reacts with 4-hydroxybenzaldehyde in a nucleophilic substitution reaction in presence of K_2CO_3.[35] The products of both steps were confirmed by ^{1}H-NMR and LCMS (Fig. 2a, b, S1 and S2†).

^{1}H-NMR (200 MHz, $CDCl_3$, ppm) of –CHO–ONB–Br showed peaks at 10.03 (s, 1H) for –CHO–Phenyl–, 8.90 (s, 1H) –CH–Phenyl–, 8.50 (d, 1H) –CH–Phenyl–, 8.10 (d, 2H) –CH–Phenyl–,

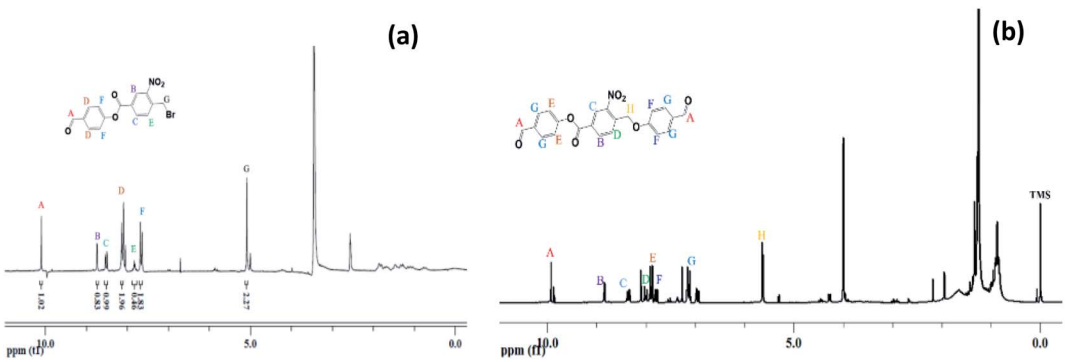

Fig. 2 (a) ^{1}H-NMR of 4-formylphenyl 4-(bromomethyl)-3-nitrobenzoate, (b) ^{1}H-NMR of 4-((4-formylphenoxy)methyl)-3-nitrobenzoate.

7.70 (d, 1H) –CH–Phenyl–,7.60 (d, 2H) –CH–Phenyl–, 4.97 (d, 2H) Br–CH_2–Phenyl–. Fig. 2a.

^{1}H-NMR (200 MHz, DMSO-d_6, ppm) was recorded for –CHO–ONB–CHO 9.98 (s, 2H, –CHO–Phenyl.–), 8.90 (s, 1H, –CH–Phenyl.–), 8.50 (d, 1H, –CH–Phenyl.–), 8.00 (d, 1H, –CH–Phenyl.–), 7.90 (d, 2H, –CH–Phenyl.–), 7.80 (d, 2H, –CH–Phenyl.–), 7.20 (d, 4H, –CH–Phenyl.–), 5.60 (s, 2H, Br–CH_2–Phenyl.–). Fig. 2b.

The LCMS data for –CHO–ONB–Br depicted the presence of characteristic bromine isotopic peaks[39] at 364 and 362 of equal intensity and the peaks for –CHO–ONB–CHO was confirmed at *m*/*z* 404.1, 405.1. Fig. S1 and S2.†

UV-responsive behaviour of crosslinked microspheres

The cleavage of ONB (*ortho*-nitro benzyl) group is a photolytic reaction which is already known. The photolabile group (ONB), when irradiated with UV radiation, yields a nitroso compound and a free acid after photocleavage.[40] Thus, the application of externally applied stimulus (UV radiation) causes physical and chemical change in the crosslinker used in the formulation of crosslinked hydrogel microspheres which may trigger effective and control release of the loaded drugs.[41] Further, the crosslinker (CHO–ONB–CHO) solution, when irradiated with UV-light, shows a visible change in absorption spectrum indicating its UV sensitive nature. The irradiated absorption spectrum of crosslinker displayed slight shifting of peaks from 310–340 nm (Fig. 4a.). Moreover, the UV sensitivity of crosslinker was visually observed by the change in the color of the crosslinker solution (Fig. 4b and c). The crosslinker was colorless before UV irradiation which changed to light yellow color after irradiation signifying UV sensitivity.

Preparation of CHO–ONB–CHO crosslinked hydrogels

Coacervation phase separation method was used to prepare chitosan hydrogels. According to this method, the formation of microspheres results from a surface phenomenon due to the interaction between a polymeric solution (chitosan solution) and a coagulant medium (2 M NaOH solution), which brings about phase separation of the polymeric microspheres. A polymer-rich coacervated phase is created on precipitation with immediate phase separation.[42] The microspheres prepared were crosslinked by treating them with CHO–ONB–CHO solution in acetone–water system with the crosslinker being soluble in acetone.

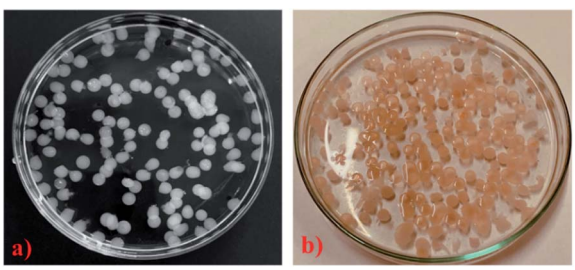

Fig. 3 (a) ONB–chitosan hydrogel microspheres in swelling condition, (b) dox loaded hydrogel in swelling state.

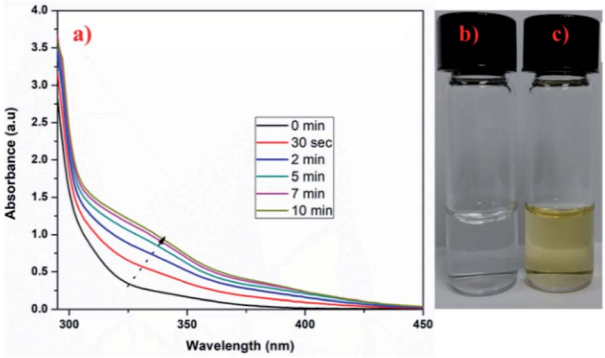

Fig. 4 (a) UV-visible spectra of irradiated crosslinker (CHO–ONB–CHO), (b) and (c) digital images of crosslinker solution before irradiation and after irradiation respectively.

The crosslinking reaction occurs between amine groups of chitosan and aldehydic groups of the crosslinker CHO–ONB–CHO resulting in the formation of the imine bonds *via* a Schiff reaction.[43] The microspheres prepared by this method were non-adherent due to addition of aluminium powder (0.03%) and magnesium silicate (0.5%) which prevents the aggregation of these microspheres.

The SEM micrographs of the pristine chitosan and ONB–chitosan crosslinked hydrogels are shown in Fig. 5(a–f). The SEM micrograph of pure chitosan analyzed at two different resolutions displayed rough surface morphology (Fig. 5(a and b)). After crosslinking of chitosan with crosslinker (CHO–ONB–CHO), microspheres with porous surfaces were obtained (Fig. 5(c–f)). Such morphology plays a significant role in controlling the swelling behavior of hydrogels as well as in sustained release of the drugs. Due to the presence of many pores on surface, the hydrogel is likely to exhibit good permeability for drug molecules and can support their loading and release properties as well. These microspheres were spherical in shape with average diameter of about 20 μm (Fig. 5c).

Structural analysis

The FTIR spectra (Fig. 6a (black trace)) shows characteristic peaks of chitosan 3429 cm^{-1} assigned to O–H stretch

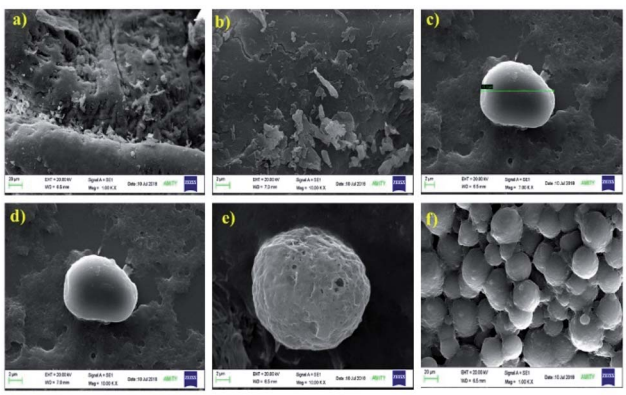

Fig. 5 SEM micrographs of (a) and (b) chitosan and (c), (d), (e) and (f) ONB–chitosan.

overlapping with N–H stretch, 2921 and 2867 cm^{-1} for C–H stretch, 1640 cm^{-1} corresponds to amide II band and C–O stretching of acetyl group. The peak at 1592 cm^{-1} is assigned to amide II band, N–H stretching. 1485–1380 cm^{-1} correspond to asymmetric C–H bending of CH_2 group and 1035 cm^{-1} bridge O stretching of glucosamine residue.[44] The spectrum for ONB–chitosan hydrogel (Fig. 6a (red trace)) showed a characteristic peaks at 2925 cm^{-1} (aromatic C–H stretching). The stretching frequency at 1517 cm^{-1} corresponds to the presence of N–O (nitro-) group. The other peaks include C=O (ester) stretching, C–O (ester) stretching at 1744 cm^{-1} and 1172 cm^{-1} respectively. The peak at 1660 cm^{-1} corresponds to C=C (aromatic) stretching frequency. One of the characteristic peaks in the spectrum occurs at 1637 cm^{-1} which is assigned to the formation of Schiff base (C=N, imine stretching) due to the reaction between the amine group of chitosan and aldehydic group the ONB-crosslinker.[42,45]

The XRD diffractograms of chitosan and crosslinked-chitosan have been analysed in the scan range of 10–80° (2θ). The chitosan shows a sharp peak at 2θ value of 20° and a minor peak at 29°. Chitosan is semi-crystalline in nature[46] and its crystallinity depends on the degree of deacetylation and the hydrogen bonding, both inter- and intra-molecular, present in chitosan due to the presence of hydroxyl and amine groups.[47] This results in a sharp peak in XRD pattern as shown in Fig. 4b (black trace). Upon crosslinking the hydrogen bonding is broken to a large extend, if not completely, and the amorphous nature prevails in the hydrogels. The appearance of a broader peak in the XRD diffractogram of ONB–chitosan hydrogels at 2θ = 19.3°, Fig. 6b (red trace), shows amorphous character of the crosslinked-chitosan after crosslinking reaction and the plausible reason being removal of hydrogen bonding.

Thermal analysis

TGA thermograms of chitosan and ONB–chitosan hydrogels recorded are displayed in Fig. 7a. The weight loss at 100 °C in chitosan and ONB–chitosan hydrogels accounts for the moisture loss and loss of some volatile contaminations.[48] The TGA/DSC of the ONB–chitosan hydrogels showed few degradation steps in the range 150–700 °C. The maximum weight loss occurs in the temperature band of 250–450 °C and the weight loss particularly around 300 °C (55.7%) attributes to the polymeric back bone degradation, which includes dehydration of the glucosidic rings, depolymerization accompanied by formation of water, CH_4 and CO_2.[49] The thermal degradation of the ONB–

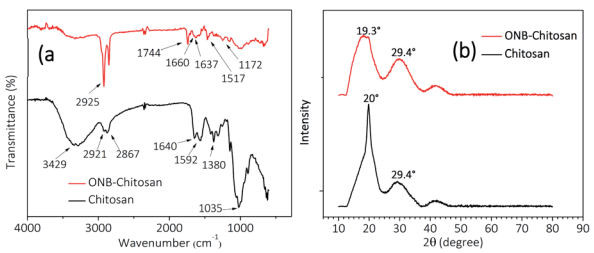

Fig. 6 (a) FTIR spectra and (b) XRD diffractograms of chitosan (black trace) and ONB-crosslinked chitosan hydrogels (red trace).

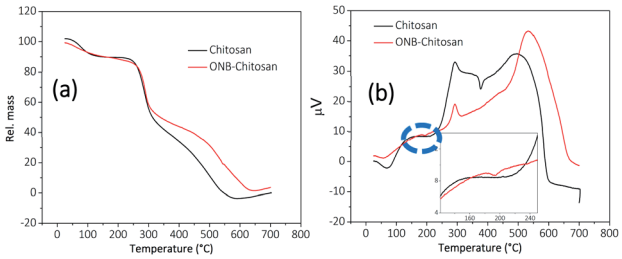

Fig. 7 (a) TGA and (b) DSC thermographs of chitosan (black trace) and ONB–chitosan hydrogels (red trace) (inset shows an exothermic peak at 193.7 °C).

chitosan hydrogels in the second step is likely to be attributed to the thermal degradation of the chitosan moiety along with the molecule destruction involving thermal oxidation of the ONB–crosslinker linked to it in a Schiff-base reaction.[50]

The weight loss of ONB–chitosan hydrogels in the temperature range of 350–500 °C becomes a slower process owing to the better thermal stability of the crosslinked hydrogels compared to the pristine chitosan.

The DSC thermograph, Fig. 7b, of the chitosan showed the glass transition temperature (T_g) in the range of 125–180 °C.[51] The exothermic peak around 70 °C and 60 °C accounted for the loss of moisture in chitosan and crosslinked-chitosan respectively. The endothermic peak for chitosan occurred at 240 °C and continued up to 314 °C owing to its thermal degradation and the maxima was observed at 293.4 °C which may correspond to the melting transition temperature.[52,53] The endothermic peak at around 500–700 °C owes to the further degradation of chitosan. This process is attributed to a series of complex processes which not only includes the depolymerization and dehydration of the saccharide units but decomposition of the chitosan units (acetylated and deacetylated) as well.[54] The exothermic peak in the chitosan thermograph at 377 °C is due to partial degradation and intermolecular disintegration of its structure[53] and the removal of the residual moisture which may be have still persisted inside the comparatively flexible rings and internal structure of chitosan. This flexibility is lost in the ONB–chitosan due crosslinking between the polymeric chains. T_g of ONB-crosslinked chitosan was not visible in the DSC. The thermal degradation of ONB–chitosan hydrogels occur at 270 °C owing to the better thermal stability due to crosslinking in chitosan. The inset in the DSC curve of ONB–crosslinked chitosan shows an exothermic peak at 193.7 °C which can be attributed to the removal of the absorbed moisture/water in the cross-linked polymeric network.[55] There is loss of the chain flexibility in the crosslinked chitosan and whatever the moisture there is in the crosslinked structure is lost at early temperatures. Thus, there is no extra exothermic peak in the thermograph of ONB–chitosan at around 350 °C unlike seen in chitosan thermograph.

Contact angle measurements

Contact angle measurements were carried out to study the surface properties of the prepared crosslinked hydrogels. As

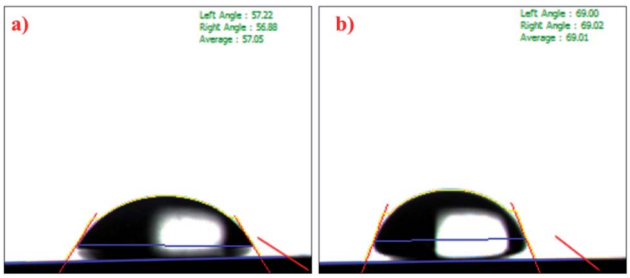

Fig. 8 Contact angle of (a) chitosan and (b) ONB–chitosan hydrogel.

shown in Fig. 8, the chitosan exhibited a contact angle of about 57.05° and that of ONB–chitosan as 69.01°. The crosslinking in chitosan resulted in increase the water contact angle, indicating decreased surface wettability. The decreased hydrophilicity in the ONB–chitosan hydrogels is due to the hydrophobic cross-linker attached to the hydrophilic chitosan backbone. Hydrogels are generally partial for the hydrophilic drugs and delivery of hydrophobic drugs becomes challenging. Incorporation of hydrophobic groups, in this case a covalently bonded cross-linker, onto a hydrophilic polymeric backbone enables the hydrogels to have a slightly better affinity for hydrophobic drugs.[56–58]

Swelling studies

The groups in the crosslinked hydrogel respond to the certain environmental stimuli like pH and will result in the change in the polymer properties like swelling–deswelling due to the change in the polymeric network. Swelling and deswelling behavior of the hydrogels occurs through water convection and is attributed to the porosity and pore-size of the gels. Chitosan hydrogels are known to have highly porous network leading to enhanced swelling ratio and in turn shorter equilibrium time.[59] The swelling behavior of prepared ONB–chitosan hydrogel hydrated at various pHs (pH 2.1, 5.7, 7.4) is shown in Fig. 9. At acidic pH of 2.1, the hydrogel showed an abrupt increase in the swelling ratio (1036%) for almost 3 hours. After 3.5 h the hydrogel started to degrade in the solution causing it to burst by the completion of 22 h. At pH 7.4, there was a slight increase in the SR (167.02%) which almost remained almost constant over the span of 27 h. The hydrogel at pH 5.7, showed a steady increase in the SR (2893.88%) over a longer period of time (22 h) without any or negligible degradation. After 22 h the hydrogel started to lose the weight and SR value started to decrease indicating its slow degradation in the solution.

As chitosan is known to be soluble in acidified water (pH < 5) due to the protonation and conversion of amino group of the chitosan into ammonium group (NH^{3+}).[60] Thus, at lower pH values there are repulsive electrostatic forces between the polymeric chains causing the hydrogel to disrupt. At higher pH (pH 7.4), NH^{3+} is deprotonated and the repulsive forces between the polymeric chains is decreased. There is an increase in the osmotic pressure inside the hydrogel network, preventing the solvent molecules to enter the matrix. Moreover, there is an increase in the inter- and intra-chain hydrogen bonded interactions. As a result of which the size of the pores is further decreased, thus, decreasing the swelling.[61] The highest swelling ratio of the ONB–chitosan hydrogel at pH 5.7 can be explained by the presence of positively charged NH^{3+} in the polymeric chain which leads to the diffusible structure and a balance between protonation and deprotonation. More water absorption is possible due to hydrogen bonding, thus, leading to the absorption of higher contents of water from the solution.

Swelling kinetics

In order to determine the kinetics of swelling, the method proposed by Quintana *et al.*[62] was adopted. For the hydrogel to follow first-order kinetics, at time t, the rate of swelling is directly depends on the water content inside the hydrogel prior to the attainment of equilibrium (defined by M_∞, equilibrium water content). The first-order swelling is then expressed by the following equation (eqn (3)):

$$dM/dt = KM_\infty \quad (3)$$

where M_t is the hydrogel water content at time t and K is the proportionality constant. Upon integration of eqn (3) between the limits, $t = 0$ to t and $M = 0$ to ∞, eqn (4) is obtained:

$$\ln(M_\infty/M_\infty - M_t) = Kt \quad (4)$$

The plot is obtained by varying as a function of time t. If the graph is a straight line, the swelling of hydrogel follows a first-

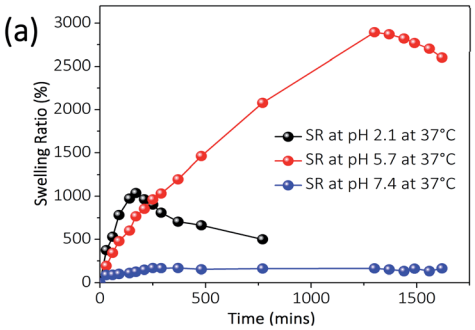

(b)

ONB-chitosan	N	K	R^2
pH 2.1	0.6145	0.044162	0.9841
pH 5.7	0.7088	0.006449	0.9966
pH 7.4	0.2533	0.209255	0.8362

Fig. 9 (a) Swelling ratio of ONB–chitosan hydrogels at pH = 2.1, 5.7 and 7.4 at 37 °C and (b) table showing various parameters obtained from swelling kinetics.

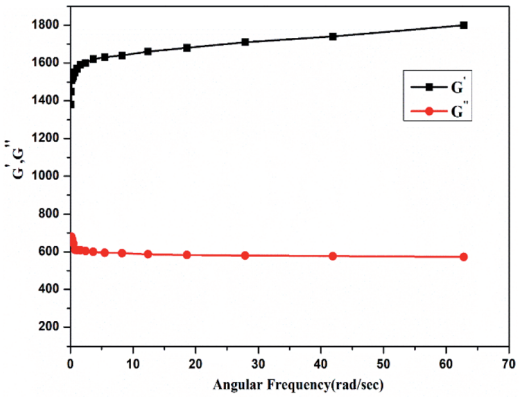

Fig. 10 Rheological analysis of crosslinked ONB–chitosan hydrogel.

order kinetic mechanism. For second order kinetics, the swelling rate at time t may be expressed as following:

$$dM/dt = K(M_\infty - M_t)^2 \quad (5)$$

Integrating eqn (5) within limits, $t = 0$ to t and $M = 0$ to M_∞, the below equation is attained:

$$t/M_t = 1/KM_\infty{}^2 + 1/M_\infty t \quad (6)$$

If the plot of t/M_t *vs.* time is a straight line, the swelling of hydrogel is a second-order kinetic mechanism with a slope of $1/M$. The swelling process of ONB–chitosan hydrogel at various pH values fits more closely to the second-order kinetic model with the regression value, R^2, values closer to 1.

The swelling behavior of the ONB–chitosan hydrogel was studied further using eqn (2) and can be categorized as Fickian (diffusion-controlled), non-Fickian (relaxation-controlled) or Case II diffusion.

After applying log on both sides of eqn (2), we get the following equation:

$$\log(M_t/M_{eq}) = \log k + n \log t \quad (7)$$

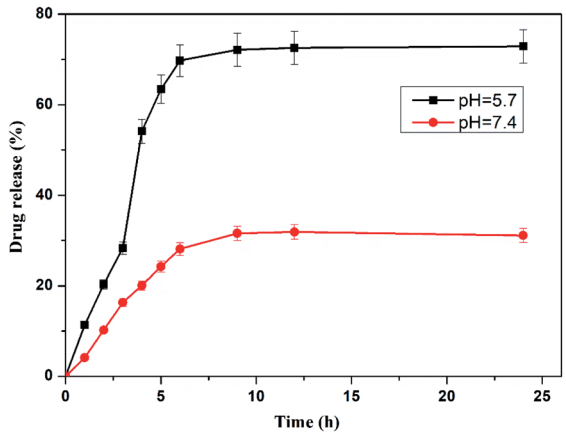

Fig. 11 % drug release plot of dox-loaded ONB-chitosan hydrogel at pH 7.4 and 5.7.

where M_t and M_{eq} are the amounts of solvent uptake at time t and at equilibrium swelling state respectively, k as the swelling rate constant of the hydrogel and n represents the swelling exponent or diffusion coefficient to define the diffusion method as well as transportation and releasing.[63,64] The solvent molecules get diffused into the hydrogel as explained by Fick's law.

The exponent n and the value k were obtained from the slope and the intercept ($\log k$), respectively, of the curve, plotted between $\ln(M_t/M_{eq})$ and $\ln t$. The results are given in Fig. 9b. The value of n indicates that the swelling mechanism of the ONB–chitosan hydrogel and was found to follow non-Fickian diffusion at pH 2.1 and 5.7 which changed to Fickian diffusion at pH 7.4. When diffusion of solvent occurs much faster than the relaxation of the polymer chains, the swelling kinetics is said to be diffusion controlled or Fickian diffusion.

Taken together the synthesized dung carrier shows dual stimuli; light and pH. The increased diffusion and swelling at pH 5.7 can be exploited for the maximum drug loading that fits well with the acidic environments of the inflammatory sites or cancerous tissues during drug release. The dual response makes the carrier highly efficient and specific and thus can be employed for the controlled release of the release of the therapeutic agents.

Rheological behavior

The dynamic mechanical properties like loss modulus (G'') and storage modulus (G') of the chitosan hydrogel are plotted against angular frequency (Fig. 10). It has been observed that the G' values of the hydrogel are higher than G'' values. The higher values of G' than G'' implies hydrogel stiff and elastic behavior. The G' values of hydrogel was found to be 1741 pa while as the values of G'' was about 573 pa. Thus, the magnitude of elastic modulus and the flatness of curve suggests the viscoelastic nature and mechanical robustness of hydrogel which can withstand solid gel like character.

Dox loading and release studies

The high loading percentage of dox was observed at pH. 5.7 (17.23%) than at 7.4 pH (8.23%) in the hydrogel. The lower loading of drug may be due to collapsing or shrinking of crosslinked hydrogel at higher pH as a result of which the hydrogel could not disseminate fast in the dox solution. The release behaviour of dox from loaded hydrogel were studied at pH of 7.4 and pH 5.7. These loaded hydrogels were dipped in 10 mL of buffer solutions of both pH. To maintain the constant volume of the dissolution media, the withdrawn release media at specific time was replaced with the fresh media. After plotting of percentage dox release against time for the crosslinked hydrogel, it was detected that the hydrogel displayed a pH responsive release behaviour showing 71.75% dox release after 24 h at pH 5.7. However, at pH 7.4 only 30.82% dox was released from the hydrogel (Fig. 11). The lower dox release behaviour of hydrogel at pH 7.4 may be ascribed to greater hydrolytic stability of Schiff base linkages at this pH. Furthermore, the higher release of dox at 5.7 pH may be due to greater swelling capacity

of crosslinked hydrogel at lower pH which has been confirmed from hydrogel swelling behavior.

Conclusion

A novel photocleavable crosslinker with UV-responsive *ortho*-nitrobenzyl moiety, was synthesized through esterification and nucleophilic substitution reactions. The synthesized crosslinker (CHO–ONB–CHO) was characterized using 1H-NMR and LCMS. This prepared dialdehyde-containing crosslinker was utilized to prepare dual-stimuli responsive chitosan hydrogel through Scihff base reaction making the hydrogels UV- as well as pH-responsive. The response to UV and pH was studied successfully. The crosslinker was found to degrade by absorption of the UV-radiation in the range of 310–340 nm wavelength. The swelling ratios (SR) of ONB–chitosan hydrogel were studied at various pH (2.1, 5.7, 7.4) and it was found that the SR is highest for pH 5.7 as compared to pH 2.1 and 7.4. The maximum swelling at 5.7 can be utilized for the maximum uptake and release of the therapeutic agents in the acidic environments of cancerous tissues, endosomes and lysosomes. Both the stimuli make the hydrogel an efficient drug-delivery system by giving us more control over the release of the therapeutic agents. The dox release studies revealed higher drug release percentage at acidic pH (5.7 pH).

Conflicts of interest

There are no conflicts to declare.

Acknowledgements

The author is thankful to the Amity University (UP, India) and Kaohsiung Medical University (Taiwan) for providing the required lab facilities.

References

1 Y. Qiu and K. Park, Environment-sensitive hydrogels for drug delivery, *Adv. Drug Delivery Rev.*, 2012, **64**, 49–60.
2 A. S. Hoffman, Stimuli-responsive polymers: biomedical applications and challenges for clinical translation, *Adv. Drug Delivery Rev.*, 2013, **65**, 10–16.
3 A. G. Lacko, M. Nair, L. Prokai and W. J. McConarthy, Prospects and challenges of the development of lipoprotein-based formulations for anti-cancer drugs, *Expert Opin. Drug Delivery*, 2007, **4**, 66–675.
4 G. E. Cinay, P. Erkoc, M. Alipour, Y. Hashimoto, Y. Sasaki, K. Akiyoshi and S. Kizilel, Nanogel-Integrated pH-Responsive Composite Hydrogels for Controlled Drug Delivery, *ACS Biomater. Sci. Eng.*, 2017, **3**, 370–380.
5 H. Liu, C. Wang, C. Li, Y. Qin, Z. Wang, F. Yang, Z. Li and J. Wang, A functional chitosan-based hydrogel as a wound dressing and drug delivery system in the treatment of wound healing, *RSC Adv.*, 2018, **8**, 7533–7549.
6 B. M. Holzapfel, J. C. Reichert, J. T. Schantz, U. Gbureck, L. Rackwitz, U. Nöth, F. Jakob, M. Rudert, J. Groll and D. W. Hutmacher, How smart do biomaterials need to be? A translational science and clinical point of view, *Adv. Drug Delivery Rev.*, 2013, **65**, 581–603.
7 Y. Zheng, L. Wang, L. Lu, Q. Wang and B. C. Benicewicz, pH and Thermal Dual-Responsive Nanoparticles for Controlled Drug Delivery with High Loading Content, *ACS Omega*, 2017, **2**, 3399–3405.
8 M. Karimi, A. Ghasemi, P. Sahandi Zangabad, R. Rahighi, S. M. Moosavi Basri, H. Mirshekari, M. Amiri, Z. Shafaei Pishabad, A. Aslani, M. Bozorgomid, D. Ghosh, A. Beyzavi, A. Vaseghi, A. R. Aref, L. Haghani, S. Bahrami and M. R. Hamblin, Smart micro/nanoparticles in stimulus-responsive drug/gene delivery systems, *Chem. Soc. Rev.*, 2016, **45**, 1457–1501.
9 K. S. Soppimath, L. H. Liu, W. Y. Seow, S. Q. Lin, R. Powell, P. Chan and Y. Y. Yang, Multifunctional core/shell nanoparticles self-assembled from pH-induced thermosensitive polymers for targeted intracellular anticancer drug delivery, *Adv. Funct. Mater.*, 2007, **17**, 355–362.
10 W. Cui, X. Lu, K. Cui, L. Niu, Y. Wei and Q. Lu, Langmuir, dual-responsive controlled drug delivery based on ionically assembled nanoparticles, *Langmuir*, 2012, **28**, 941–9420.
11 W. H. Chiang, V. T. Ho, W. C. Huang, Y. F. Huang, C. S. Chern and H. C. Chiu, Dual stimuli-responsive polymeric hollow nanogels designed as carriers for intracellular triggered drug release, *Langmuir*, 2012, **28**, 15056–15064.
12 J. Zhang, L. Wu, F. Meng, Z. Wang, C. Deng, H. Liu and Z. Zhong, pH and reduction dual-bio responsive polymersomes for efficient intracellular protein delivery, *Langmuir*, 2012, **28**, 2056–2065.
13 B. Remant, B. Thapa and P. Xu, pH and redox dual responsive nanoparticle for nuclear targeted drug delivery, *Mol. Pharm.*, 2012, **9**, 2719–2729.
14 S. Yoon, W. J. Kim and H. S. Yoo, Dual-responsive breakdown of nanostructures with high doxorubicin payload for apoptotic anticancer therapy, *Small*, 2013, **9**, 284–293.
15 H. R. Zhao, K. Wang, Y. Zhao and L. Q. Pan, Novel sustained-release implant of herb extract using chitosan, *Biomaterials*, 2002, **23**, 4459–4462.
16 S. Yu, G. Wu, X. Gu, J. Wang, Y. Wang, H. Gao and J. Ma, Magnetic and pH-sensitive nanoparticles for antitumor drug delivery, *Colloids Surf., B*, 2013, **103**, 15–22.
17 Y. Z. You, C. Y. Hong and C. Y. Pan, Facile one-pot approach for preparing dually responsive core–shell nanostructure, *Macromolecules*, 2009, **42**, 573–575.
18 J. Tan, H. Kang, R. Liu, D. Wang, X. Jin, Q. Li and Y. Huang, pH-sensitive vesicles based on a biocompatible zwitterionic diblock copolymer, *Polym. Chem.*, 2011, **2**, 672–678.
19 X. Sui, X. Feng, A. Di Luca, C. A. Van Blitterswijk, L. Moroni, M. A. Hempenius and G. J. Vancso, Poly(*N*-isopropylacrylamide)–poly(ferrocenylsilane) dual-responsive hydrogels: synthesis, characterization and antimicrobial applications, *Polym. Chem.*, 2013, **4**, 337–342.

20 W. Chen, F. Meng, F. Li, S. J. Ji and Z. Zhong, pH-responsive biodegradable micelles based on acid-labile polycarbonate hydrophobe: synthesis and triggered drug release, *Biomacromolecules*, 2009, **10**, 1727–1735.

21 J. Du, Y. Tang, A. L. Lewis and S. P. Armes, pH-sensitive vesicles based on a biocompatible zwitterionic diblock copolymer, *J. Am. Chem. Soc.*, 2005, **127**, 17982–17983.

22 D. V. Volodkin, A. G. Skirtach and H. Möhwald, Near-IR remote release from assemblies of liposomes and nanoparticles, *Angew. Chem., Int. Ed.*, 2009, **48**, 1807–1809.

23 M. Mu, X. Li, A. Tong and G. Guo, Multi-functional chitosan-based smart hydrogels mediated biomedical application, *Expert Opin. Drug Delivery*, 2019, **16**, 239–250.

24 T. Kean and M. Thanou, Biodegradation, biodistribution and toxicity of chitosan, *Adv. Drug Delivery Rev.*, 2010, **62**, 3–11.

25 S. A. Agnihotri, N. N. Mallikarjuna and T. M. Aminabhavi, Recent advances on chitosan-based micro- and nanoparticles in drug delivery, *J. Controlled Release*, 2004, **100**, 5–28.

26 H. Tozaki, J. Komoike, C. Tada, T. Maruyama, A. Terabe, T. Suzuki, A. Yamamoto and S. Muranishi, Chitosan Capsule for colon-specific drug delivery: improvement of insulin absorption from the rat colon, *J. Pharm. Sci.*, 1997, **86**, 1016–1021.

27 W. Paul and C. P. Sharma, Chitosan, a drug carrier for the 21st century, *STP Pharma Sci.*, 2000, **10**, 5–22.

28 H. R. Zhao, K. Wang, Y. Zhao and L. Q. Pan, Novel sustained-release implant of herb extract using chitosan, *Biomaterials*, 2002, **23**, 4459–4462.

29 H. S. Kas, Chitosan: properties, preparations and application to microparticulate systems, *J. Microencapsulation*, 1997, **14**, 689–771.

30 S. B. Ross-Murphy, Rheological characterization of polymer gels and networks, *Polym. Gels Networks*, 1994, **2**, 229–237.

31 C. Zhang, Z. Liu, Z. Shi, T. Li, H. Xu, X. Ma, J. Yin and M. Tian, Inspired by elastomers: fabrication of hydrogels with tunable properties and re-shaping ability *via* photo-crosslinking at a macromolecular level, *Polym. Chem.*, 2017, **8**, 1824–1832.

32 M. J. Moura, H. Faneca, M. P. Lima, M. H. Gil and M. M. Figueiredo, In situ forming chitosan hydrogels prepared *via* ionic/covalent Co-crosslinking, *Biomacromolecules*, 2011, **12**, 3275–3284.

33 H. Basan, M. Gümüşderelíoğlu and T. Orbey, Diclofenac sodium releasing pH-sensitive monolithic devices, *Int. J. Pharm.*, 2002, **245**, 191–198.

34 X. Zhao, J. Chen, Y. Zeng, Y. Li, Y. Han and Y. Li, Photoinduced electron transfer within porphyrin-anthraquinone dyads connected by Hamilton hydrogen bonding, *Chin. J. Chem.*, 2010, **28**, 1580–1586.

35 K. S. Li, P. Xiao, D. L. Zhang, X. Ben Hou, L. Ge, D. X. Yang, H. Da Liu, D. F. He, X. Chen, K. R. Han, X. Y. Song, X. Yu, H. Fang and J. P. Sun, Identification of para-Substituted Benzoic Acid Derivatives as Potent Inhibitors of the Protein Phosphatase Slingshot, *ChemMedChem*, 2015, **10**, 1980–1987.

36 V. L. Gonçalves, M. C. M. Laranjeira, V. T. Fávere and R. C. Pedrosa, Effect of crosslinking agents on chitosan microspheres in controlled release of diclofenac sodium, *Polímeros*, 2005, **15**, 6–12.

37 A. H. Pandit, N. Mazumdar, K. Imtiaz, M. M. A. Rizvi and S. Ahmad, Periodate-Modified Gum Arabic Cross-linked PVA Hydrogels: A Promising Approach toward Photoprotection and Sustained Delivery of Folic Acid, *ACS Omega*, 2019, **14**, 16026–16036.

38 P. L. Ritger and N. A. Peppas, A simple equation for description of solute release II. Fickian and anomalous release from swellable devices, *J. Controlled Release*, 1987, **5**, 37–42.

39 T. De Vijlder, D. Valkenborg, F. Lemière, E. P. Romijn, K. Laukens and F. Cuyckens, A tutorial in small molecule identification *via* electrospray ionization-mass spectrometry: the practical art of structural elucidation, *Mass Spectrom. Rev.*, 2018, **37**, 607–629.

40 P. Wang, Photolabile protecting groups: structure and reactivity, *Asian J. Org. Chem.*, 2013, **2**, 452–464.

41 G. Jalani, R. Naccache, D. H. Rosenzweig, L. Haglund, F. Vetrone and M. Cerruti, Photocleavable hydrogel-coated upconverting nanoparticles: a multifunctional theranostic platform for NIR imaging and on-demand macromolecular delivery, *J. Am. Chem. Soc.*, 2016, **138**, 1078–1083.

42 W. S. W. Ngah, C. S. Endud and R. Mayanar, Removal of copper(II) ions from aqueous solution onto chitosan and cross-linked chitosan beads, *React. Funct. Polym.*, 2002, **50**, 181–190.

43 R. M. Issa, A. M. Khedr and H. Rizk, H NMR, IR and UV/VIS spectroscopic studies of some Schiff bases derived from 2-aminobenzothiazole and 2-amino-3-hydroxypyridine, *J. Chin. Chem. Soc.*, 2008, **55**, 875–884.

44 J. Singh, P. K. Dutta, J. Dutta, A. J. Hunt, D. J. Macquarrie and J. H. Clark, Preparation and properties of highly soluble chitosan-l-glutamic acid aerogel derivative, *Carbohydr. Polym.*, 2009, **76**, 188–195.

45 S. Kumar and J. Koh, Physio-chemical, optical and biological activity of chitosan-chromone derivative for biomedical applications, *Int. J. Mol. Sci.*, 2012, **13**, 6103–6116.

46 S. J. Kim, S. R. Shin, G. M. Spinks, I. Y. Kim and S. I. Kim, Synthesis and characteristics of a semi-interpenetrating polymer network based on chitosan/polyaniline under different pH conditions, *J. Appl. Polym. Sci.*, 2005, **96**, 867–873.

47 M. Chen, T. Runge, L. Wang, R. Li, J. Feng, X. L. Shu and Q. S. Shi, Hydrogen bonding impact on chitosan plasticization, *Carbohydr. Polym.*, 2018, **200**, 115–121.

48 I. Corazzari, R. Nisticò, F. Turci, M. G. Faga, F. Franzoso, S. Tabasso and G. Magnacca, Advanced physico-chemical characterization of chitosan by means of TGA coupled on-line with FTIR and GCMS: Thermal degradation and water adsorption capacity, *Polym. Degrad. Stab.*, 2015, **112**, 1–9.

49 N. Işiklan, F. Kurşun and M. Inal, Graft copolymerization of itaconic acid onto sodium alginate using benzoyl peroxide, *Carbohydr. Polym.*, 2010, **79**, 665–672.

50 I. Ledeţi, A. Alexa, V. Bercean, G. Vlase, T. Vlase, L. M. Şuta and A. Fuliaş, Synthesis and degradation of Schiff bases containing heterocyclic pharmacophore, *Int. J. Mol. Sci.*, 2015, **16**, 1711–1727.

51 S. Argin-Soysal, P. Kofinas and Y. M. Lo, Effect of complexation conditions on xanthan-chitosan polyelectrolyte complex gels, *Food Hydrocolloids*, 2009, **23**, 202–209.

52 A. H. Gedam and R. S. Dongre, Adsorption characterization of Pb(II) ions onto iodate doped chitosan composite, *RSC Adv.*, 2015, **5**, 54188–54201.

53 S. Parvez, M. M. Rahman, M. A. Khan, M. A. H. Khan, J. M. M. Islam, M. Ahmed, M. F. Rahman and B. Ahmed, Preparation and characterization of artificial skin using chitosan and gelatin composites for potential biomedical application, *Polym. Bull.*, 2012, **69**, 715–731.

54 C. H. Chen, F. Y. Wang, C. F. Mao and C. H. Yang, Studies of Chitosan. Preparation and Characterization of Chitosan/Poly(vinyl alcohol) Blend Films, *J. Appl. Polym. Sci.*, 2007, **105**, 1086–1092.

55 A. A. Aldana, R. Toselli, M. C. Strumia and M. Martinelli, J. Chitosan films modified selectively on one side with dendritic molecules, *Mater. Chem.*, 2012, **22**, 22670–22677.

56 E. Larrañeta, S. Stewart, M. Ervine, R. Al-Kasasbeh and R. F. Donnelly, Hydrogels for hydrophobic drug delivery. Classification, synthesis and applications, *J. Funct. Biomater.*, 2018, **9**, 13.

57 J. J. Pillai, A. K. T. Thulasidasan, R. J. Anto, D. N. Chithralekha, A. Narayanan and G. S. V. Kumar, Folic acid conjugated cross-linked acrylic polymer (FA-CLAP) hydrogel for site specific delivery of hydrophobic drugs to cancer cells, *J. Nanobiotechnol.*, 2014, **12**, 25.

58 M. McKenzie, D. Betts, A. Suh, K. Bui, L. D. Kim and H. Cho, Hydrogel-based drug delivery systems for poorly water-soluble drugs, *Molecules*, 2015, **20**, 20397–20408.

59 R. Ahmadi and J. D. De Bruijn, Biocompatibility and gelation of chitosan-glycerol phosphate hydrogels, *J. Biomed. Mater. Res., Part A*, 2008, **86**, 824–832.

60 A. Islam and T. Yasin, Controlled delivery of drug from pH sensitive chitosan/poly(vinyl alcohol) blend, *Carbohydr. Polym.*, 2012, **88**, 1055–1060.

61 M. Shibayama and T. Tanaka, Volume phase transition and related phenomena of polymer gels, *Adv. Polym. Sci.*, 1993, **109**, 1–62.

62 J. R. Quintana, N. E. Valderruten and I. Katime, Synthesis and swelling kinetics of poly(dimethylaminoethyl acrylate methyl chloride quaternary-co-itaconic acid) hydrogels, *Langmuir*, 1999, **15**, 4728–4730.

63 L. Brannon-Peppas and N. A. Peppas, Dynamic and equilibrium swelling behaviour of pH-sensitive hydrogels containing 2-hydroxyethyl methacrylate, in *The Biomaterials: Silver Jubilee Compendium*, 1990, pp. 51–60.

64 S. Swarnalatha, R. Gopi, A. Ganesh Kumar, P. K. Selvi and G. Sekaran, A novel amphiphilic nano hydrogel using ketene-based polyester with polyacrylamide for controlled drug delivery system, *J. Mater. Sci.: Mater. Med.*, 2008, **19**, 3005–3014.

